Phytopathologia Mediterranea (2016) 55, 2, 172–183
DOI: 10.14601/Phytopathol_Mediterr-16093

RESEARCH PAPERS

Combined expression of p20 and p23 proteins from *Citrus tristeza virus* show enhanced local silencing suppressor activity

Ângela A. COSTA[1], Tatiana R. MARTINS[2], Natália T. MARQUES[3] and Gustavo NOLASCO[1]

[1] Centre for Mediterranean Bioresources and Food (MeditBio), Faculdade de Ciências e Tecnologia, Universidade do Algarve, Campus de Gambelas, 8005-139, Faro, Portugal
[2] Universidade do Algarve, Campus de Gambelas, 8005-139 Faro, Portugal
[3] Center for Electronics, Optoelectronics and Telecommunications (CEOT), Faculdade de Ciências e Tecnologia, Universidade do Algarve, Campus de Gambelas, 8005-139, Faro, Portugal

Summary. Viruses developed a strategy to counter-defence the posttranscriptional gene silencing mechanism (PTGS) based on the activity of silencing suppressor proteins. *Citrus tristeza virus* (CTV), a member of the genus *Closterovirus*, has two suppressor proteins (p20 and p23) that target the local RNA silencing response of the host. In GFP transient co-expression assays performed on *Nicotiana benthamiana* 16C plants, local suppressor activity of p23 and p20 was similar. Co-expression of both proteins from a mild or a stem pitting CTV isolate showed stronger local suppression activity than either suppressor alone, with an increased GFP transcript level six- (for Gp M) to nine-fold (for Gp 3a) higher than non-inoculated 16C plants, in parallel with low accumulation of siRNAs. Further, GFP brightness of leaves infiltrated with *Agrobacterium* cultures at an OD_{600} of 0.5 was comparable to those infiltrated with OD_{600} 0.25. These findings indicate that combined action of p20 and p23 proteins results in enhanced suppressor activity.

Key words: RNA silencing, Virus suppressor, siRNA, GFP, Closterovirus.

Introduction

RNA interference results in specific gene silencing by small RNAs, such as microRNAs (miRNAs) and small interfering RNAs (siRNAs). This regulates a wide range of biological processes including virus resistance and host gene expression (Diaz-Pendon and Ding, 2008). These mechanisms of RNA silencing are ancient cellular defence pathways conserved among eukaryotes (Szittya *et al*., 2008; Alvarado and Scholthof, 2009). In plants, the defence systems against viruses involve formation of small interfering RNAs (siRNAs) that guide to sequence-specific degradation of the corresponding mRNAs, leading to post transcriptional gene silencing (PTGS) (Voinnet, 2001; Baulcombe, 2004; Herr and Baulcombe, 2004; Ding, 2010). Initially the host cells sense the presence of double-stranded RNA (dsRNA) commonly generated during plant virus replication, and use RNase III-like enzymes known as Dicer (DCL) to produce 21-24 bp siRNAs. Subsequently the siRNA/DCL complex is converted to an active RNA induced silencing complex (RISC) containing an Argonaute (AGO) protein, which mediates the sequence-specific digestion of homologue RNA and translation repression (Burgyán, 2008). RNA silencing is non-cell autonomous in plants, by producing a mobile RNA signal that can be transported cell to cell through the plasmodesmata and long distance through phloem (Himber *et al*., 2003; Diaz-Pendon and Ding, 2008). In certain instances the cycle is self-perpetuated by the action of the RNA dependent RNA polymerase (RDR) that amplifies the silencing signal (MacDiarmid, 2005; Alvarado and Scholthof, 2009).

Corresponding author: N.T. Marques
E-mail: nmarques@ualg.pt

ISSN (print): 0031-9465
ISSN (online): 1593-2095
www.fupress.com/pm

Plant viruses overcome the host's surveillance system by encoding viral suppressors of RNA silencing (VSR) that can interfere with one or more steps of the PTGS pathway (Alvarado and Scholthof, 2009). These suppressor proteins were identified in almost all viral genomes. They share no sequence similarity, are structurally diverse and target different steps of the host PTGS pathway (Burgyán, 2008; Diaz-Pendon and Ding, 2008; Burgyán and Havelda, 2011). Some viral suppressors bind to dsRNAs and inhibit its processing into siRNAs (Silhavy *et al*., 2002; Merai *et al*., 2006). Others eliminate the siRNAs or interfere with their incorporation into the RISC (Yaegashi *et al*., 2007; Diaz-Pendon and Ding, 2008; Pallas and García, 2011; Rawlings *et al*. 2011; Valli *et al*. 2011; Yoon *et al*., 2012), block the silencing signal amplification (Glick *et al*., 2008), or even interact with various enzymes and proteins as Dicer (Azevedo *et al*., 2010) or Argonaute (Alvarado and Scholthof, 2009; Giner *et* al., 2010). These suppressors span their activity to almost the complete PTGS pathway. In addition, many of them also interfere on the miRNA pathway (Kasschau *et al*., 2003, Schott *et al*., 2012). Some virus encoding miRNAs are also transcribed from suppressor gene regions (Maghuly *et al*., 2014). Moreover, several suppressor proteins have other roles in viral infection, including reduction of virus replication, control of virus movement during systemic infection (Yaegashi *et al*., 2007; Diaz-Pendon and Ding, 2008) or interference in host metabolism (Burgyán and Havelda., 2011; Pallas and García, 2011). These findings imply variable functions for these suppressors of virus infection.

Despite the substantial knowledge on how viruses counter-defence the plant antiviral strategy, the molecular mechanisms by which they suppress RNA silencing remain unclear for the majority. Furthermore, a multiple component strategy of encoding more than one suppressor has been reported for some viruses (Lu *et al*., 2004; Canizares *et al*., 2008; Ding, 2010; Senshu *et al*., 2011]. *Citrus tristeza virus* (CTV), a member of genus *Closterovirus* with a positive single stranded RNA with 19.3 kb (Karasev *et al*., 1995; Flores *et al*., 2013), encodes three proteins, p20, p23 and p25 (CP), that act as RNA silencing suppressors in *Nicotiana benthamiana* plants (Lu *et al*., 2004). Protein P25 (CP) is responsible for the encapsidation of about 97% of the RNA genome of CTV, and is also involved in CTV movement (Satyanarayana *et al*., 2000; Dolja *et al*., 2006). Protein p23 inhibits intracellular silencing, CP suppresses intercellular silencing and p20 targets both levels (Lu *et al*., 2004).

CTV p20 and p23 suppressor activities, which have been characterized before (Lu *et al*., 2004; Ruiz-Ruiz *et al*., 2011; Marques *et al*., 2012; Ruiz-Ruiz *et al*., 2013; Costa *et al*., 2014), have also other functions upon viral infection. P20, one of the more abundantly produced CTV proteins, accumulates in cytoplasm of infected cells as inclusion bodies (Gowda *et al*., 2000). Gene constructs encoding p20 to be expressed as an intron-hairpin were able to confer CTV resistance/tolerance in sour orange against stem pitting and seedling yellows isolates (Chun-zen *et al*., 2015). P23 has no homologous sequence in the Closterovirus family, and several functions are now attributed to this unique protein that is the most highly expressed, based on the relative levels of sgRNAs of CTV (Navas-Castillo *et al*., 1997). P23 is an RNA binding protein required to control asymmetric accumulation of CTV RNAs by down-regulating negative strands of genomic and sgRNAs during replication (López *et al*., 2000; Satyanarayana *et al*., 2002). P23 was reported as a pathogenicity determinant when expressed ectopically in several transgenic citrus plants with elicitation of CTV-like symptoms (Fagoaga *et al*. 2005; Ghorbel *et al*. 2001). Studies in Mexican lime, sour orange and Duncan grapefruit associated the seedling yellows syndrome to p23 and 3´UTR nucleotide sequences (Albiach-Martí *et al*., 2010). When p23 was expressed in Mexican lime under the control of a phloem-specific promoter, it induced vein clearing and stem pitting symptoms (Soler *et al*., 2015). Further, it was shown that p23 N-terminal 157 amino-acid fragment is a putative zinc finger domain flanked by motifs rich in basic amino acids, a region linked to the development of syndromes (Ruiz-Ruiz *et al*., 2013). The finding that p23 protein accumulates in cell nucleoli explains some of its functions, while its presence in plasmodesmata (Ruiz-Ruiz *et al*., 2013) is consistent with its involvement in cell-to-cell and long distance movement of the virus in phloem and phloem-associated cells, enhancing systemic infection and virus accumulation, as was observed in transgenic sour orange (Fagoaga *et al*., 2011).

When a CTV infection is established, the activated host RNAi cannot inhibit viral accumulation and systemic infection. As well, the three silencing suppressors are not able to completely block the RNAi pathway, with presence of CTV small RNAs mapped

preferentially at the 3´ terminal region of the RNA genome (Ruiz-Ruiz *et al*., 2011). The virus usually guarantees its progression in citrus plants, establishing differentially for each distinct host, without causing plant death, leading to several syndromes (Fagoaga *et al*., 2011). Therefore, the presence of three suppressors is probably essential to protect such a large genome from the antiviral silencing machinery of citrus plants.

The severity of symptoms caused by CTV in *Citrus* plants depends on the virus isolate and the combination of variety / rootstock infected, and may vary from mild or asymptomatic to more severe as seedling yellows, stem pitting or quick decline (Moreno *et al*., 2008; Nolasco *et al*., 2009). In the present study the suppression activity of CTV proteins p20 and p23 was assayed, from a mild and a stem pitting isolate, which belong to distinct phylogenetic groups (Nolasco *et al*., 2009). These groups, previously defined based on the CP gene from isolates of diverse worldwide origins, and each related to specific symptoms in indicator plants (Nolasco *et al*., 2009), maintain their pattern of clustering throughout the entire 3′-end coding region (Silva, 2011).

Both CTV p20 and p23 proteins target the local RNA silencing mechanism. To evaluate its suppressor activity, single or double expression of suppressors from the same isolate were analysed by the classical GFP transient co-expression assay in *N. benthamiana* 16C plants (Brigneti *et al*., 1998). Local suppressor activity of p23 and p20 was shown to be similar. Transient co-expression of double CTV viral suppressors from the same isolate was stronger than either suppressor alone, with down-regulation of host silencing response in *N. benthamiana* 16C evidenced by an increase in the transient expression of GFP in parallel with low accumulation of siRNAs.

Materials and methods

Plasmid construction

Cloned CTV p23 and p20 genes from CTV isolates belonging to phylogenetic groups 3a and M (Nolasco *et al*., 2009) (Table 1) available in the laboratory, were amplified and re-cloned into the binary vector pK7WG2 under the promoter CaMV 35S (Karimi *et al*., 2002), as previously described (Marques *et al*., 2012; Costa *et al*., 2014). As positive control, the 2b suppressor of *Tomato aspermy virus* (TAV) was used, provided by Dr Garcia-Arenal (Universidad Politécnica de Madrid, Spain). To induce silencing, the GFP fluorescent gene (m-gfp5-ER) (Haseloff *et al*., 1997) was used. Both were previously cloned into pK7WG2 (Costa *et al*., 2014). These constructs will in the following be named as pK-GFP, pK-p20, pK-p23 and pK-Tav-2b. The resulting binary vectors were transferred into competent cells of *Agrobacterium tumefaciens* strain C58C1, carrying the pMP90 plasmid. This confers resistance to gentamycin. Antibiotic selection was achieved using gentamycin, spectinomycin and rifampicin at 50 μg mL^{-1}. *A. tumefaciens* cultures were grown on LB medium supplemented with 10 mM MES and 20 μM acetosyringone at 28°C until reaching an OD_{600} of 0.5. The cells were centrifuged and re-suspended in 10 mM $MgCl_2$, 10 mM MES and 100 μM acetosyringone at pH 5.6, and kept at 25°C for at least 1 h before the infiltration process (Brigneti *et al*., 1998).

Table 1. Origin of the CTV isolates and associated syndromes.

Phylogenetic group	Gene	Origin of the CTV isolate	Clone name	Syndrome associated [(1)]
3a	*p20*	Madeira island	11.4	QD + SwO-SP (severe)
	p23		11.5	
M	*p20*	Spain	25.11	M
	p23		25.4	

[(1)] QD: Quick decline of trees grafted onto sour orange; SwO-SP: Stem pitting in sweet orange trees. M: Mild symptoms in indicator plant Mexican lime; absence of symptoms in sweet orange trees.

Plant material and transient expression assays

GFP transgenic 16C line of *N. benthamiana* plants, provided by Dr Sir David Baulcombe (Sainsbury Laboratory, Norwich, UK), constitutively expressing the *gfp* gene, were used for the transient expression assays with *A. tumefaciens* infiltration at four leaf stage using a 1-mL needleless syringe, as described by Brigneti *et al*. (1998). Leaves were infiltrated with the *A. tumefaciens* C58C1 cultures at OD_{600} 0.5 carrying each construct, in single or combined infiltrations.

Four modalities were assayed: 1) single infiltration with pK-GFP from a suspension of 15 mL of *A. tumefaciens*; 2) co-infiltration of pK-GFP with pK-Tav-2b; 3) co-infiltration of pK-GFP with each of the pK-20 or pK-p23 constructs; equal volumes (15:15 mL) of *Agrobacterium* cultures carrying each pK-suppressor and pK-GFP were centrifuged and re-suspended in the final volume of 15 mL; and 4) co-infiltration of pK-GFP with pK-p20 plus pK-p23 of the same isolate. For co-infiltrations of two distinct *A. tumefaciens* cultures each carrying a suppressor, equal volumes (15 mL) of individual suspension cultures at an OD_{600} 0.5 were mixed with pK-GFP (1:1:1), centrifuged and re-suspended in the same final volume (15 mL) as the single infiltration condition. The same procedure was conducted with *A. tumefaciens* cultures at OD_{600} of 0.25. Usually two leaves per plant, and ten plants assayed per each modality, were infiltrated in each experiment. Plants were observed during 9 days post infiltration (dpi). This experiment was repeated twice.

The GFP fluorescence of infiltrated leaves and whole plants was observed under long-wavelength UV light (Black Ray model B 100AP, UV Products) and photographed with a Canon EOS 450D digital camera. All images were edited using Adobe Photoshop CS3 software (Adobe Systems). GFP images from 5 dpi were converted to graytone using the Photoshop CS3 with an algorithm that converts red areas in dark areas while green and yellow were converted to lighter areas. The same algorithm was used in all images. To obtain a rough estimate of GFP fluorescence intensity, the darker areas were adjusted to similar values while the overall contrast of the images was maintained. The mean values of light and gray areas were measured and recorded. Since values for red intensity (darker areas) were approximately the same, the GFP fluorescence (white areas) could be compared between conditions.

RNA isolation and analysis

Extraction of total RNA from infiltrated leaf patches (approx. 0.7 g) at 5 and 9 dpi for Northern blot assay was performed with TRI-reagent® (Sigma), according to the supplier's protocol. The quality and concentration of all RNA preparations were determined by Nanodrop 2000 (Thermo Scientific). Total RNA from inoculated leaves of each condition (approx. 10 mg) was isolated and fractionated by electrophoresis on a 15% polyacrylamide (19:1) 7 M urea mini-gel (85 mm / 65 mm / 0.75 mm) running in TBE buffer for GFP siRNAs detection, performed as previously described (Costa *et al*., 2014). A synthetic 24-nt RNA (Pho-AGAACGGCAUCAAAGCCAACUUCA) complementary to the GFP sequence was used as a size marker. The half upper part of the gel was cut and used as a loading of 5S RNA bands. siRNAs detection was carried out on the lower part of the gel by transfer to an Amersham Hybond™-NX membrane (GE Healthcare) with an electroblotter LKB Multiphor II Novablot (Pharmacia) for 20 min, at 4 $mA.cm^{-2}$. Cross-linking of RNA was done with EDC as described in Pall *et al*. (2007). Hybridization was performed overnight at 40°C with a digoxigenin (DIG)-labeled DNA GFP-specific probe obtained by PCR amplification of the entire GFP gene. RNA blots were revealed by chemiluminescent detection with the CDP-star (Roche Applied Science), and the signal was recorded using an adapted astronomical Starlight Xpress MX7C CCD camera. This analysis was repeated twice.

For quantification of GFP expression, total RNA was extracted from infiltrated leaves using E.Z.N.A.™ Plant Kit (Omega Bio-tek) and treated with TURBO DNA-free™ kit (Ambion), according to the manufacturer's procedure. Quantitative assays of GFP mRNA for each condition were estimated by real-time RT-PCR (qRT-PCR) by means of Pfaffl method (Pfaffl, 2001). qRT-PCR was carried out with iCycler IQ (Bio-Rad) with 20 ng of each sample, using the iScript™ One-Step RT-PCR with SYBR-Green Kit (Bio-Rad). Each condition was analyzed from three leaves of distinct plants. The *N. benthamiana* ubiquitin endogenous gene expression was used as an internal standard, amplified with primer pairs ubi3 and ubi3B (Rotenberg *et al*., 2006) and cycling conditions described previously (Marques *et al*., 2012). The amplification's efficiencies were determined for GFP and ubiquitin using a six point serial dilution. Each plant sample was analysed in duplicate in three independent real-time RT-PCR assays.

An expression value of 1 was arbitrarily assigned in each experiment to the non-infiltrated *N. benthamiana* 16C line and the rest of the values were referred to this value. Statistical comparisons were made with a one-way ANOVA followed by a Tukey post-hoc test and the level of significance was set at $P<0.05$, using the IBM SPSS statistics software version 23.

Results

Suppressor activity of p20 and p23 proteins

Local transient expression assays were performed on transgenic 16C line *N. benthamiana* plants by co-infiltrations of each p20 or p23 or both CTV suppressors. The assayed p20 variants have a pairwise identity of amino acid sequences of 94.5%, and for p23 of 90%. Silencing of GFP was induced through leaf infiltration of the pK-GFP construct that expresses a transcript homologous to the transgene of 16C plants. Leaves infiltrated with the silencing inducer pK-GFP showed an increase in the GFP fluorescence at 3 dpi due to transient GFP expression (Figure 1A, GFP 3 dpi), then at 5 dpi fluorescence decreased (Figure 1A, GFP 5 dpi) and at 6 dpi had almost disappeared. The spread of the short-range silencing signal causes shutting down of GFP transgene expression, which was noticeable by a narrow red ring around the infiltrated patch, visible from 5 dpi (Figure 1A, arrows). Local silencing also began at 5 dpi, with the development of a red colouration on the infiltrated leaf patch, and at 9 dpi established red colouration was visible under UV light (Figure 1A). The systemic silencing began to develop at 7 dpi, and at 9 dpi has spread in veins dispersed over entire leaves (Figure 1A). This progressed until intense red colour (under UV) extended to the whole leaf (data not shown). The assayed VSRs were co-infiltrated with the silencing inducer pK-GFP. Patches expressing the strong suppressor Tav-2b showed bright GFP fluorescence at least for 9 dpi (Figure 1B, TAV). As expected, the co-expression of pK-GFP and each CTV VSR also maintained the GFP transient expression for a longer time, at least up to 7 dpi, confirming previously reported data for p20 and p23 (Marques *et al*., 2012; Costa *et al*., 2014). No apparent differences were found on local silencing development between leaves infiltrated with p23 or p20 of the same isolate. On the other hand, dissimilarities were found between mild and severe isolates. Suppressors p20 and p23 from Gp 3a (stem pitting isolate) (Figure 1B, p20 3a, p23 3a) depicted a more intense activity at 5 dpi, while those from Gp M (mild) showed weaker GFP fluorescence (Figure 1B, p20 M, p23 M). Double-infiltration of p20 and p23 from the same isolate with pK-GFP enhanced GFP fluorescence for both CTV groups (Gp 3a and M) (Figure 1B, p20+p23 3a, p20+p23 M), albeit for group M the greenish patch, for most plants, was slightly less intense compared with group 3a. The red ring was seen from 5 dpi on leaves co-infiltrated with p23 of both CTV groups. On the other way, expression of p20, either singly or co-inoculated with p23, caused a delay in the spread of the short-range silencing signal until 8-9 dpi for all modalities tested. At 9 dpi, less GFP fluorescence was observed for all single suppressor infiltrations (Figure 1C, p20 3a, p23 3a, p20 M, p23 M). The red ring was still not observed in many double suppressor co-infiltrated leaves and its absence coincided with a remaining bright GFP fluorescence at the inoculated patch, a pattern similar to the positive control Tav-2b (Figure 1C, p20+p23 3a, p20+p23 M, TAV). Monitoring the upper non-infiltrated leaves showed that the systemic silencing at 9 dpi was detected for all conditions tested, while not visible in all plants. In general the progression of the systemic silencing was blocked slightly more by p20 than by p23. Thus, while both CTV suppressors were able to locally suppress PTGS, none were able to suppress short-range or systemic silencing, even when combined.

Consistent with visual observations, qRT-PCR at 5 dpi shows a great reduction in the GFP mRNA levels on patches single inoculated with pK-GFP as compared to the non-inoculated 16C leaves (Figure 2A). As expected, increased GFP transcript levels were observed in patches expressing the p20 or p23 proteins alone, with exception for group p23M (Figure 2A). The combined suppressor infiltration (pK-p20 plus pK-p23) also increased GFP mRNA accumulation, generating a relative expression 6 (for group M) to 9-fold (for group 3a) greater than leaves 16C not inoculated. The one-way ANOVA performed with data of qRT-PCR confirmed that there were statistically significant differences between groups. A Tukey post-hoc test revealed that expression of GFP mRNA on leaves inoculated with pK-p20 plus pK-p23 3a, at 5 dpi, was significantly greater compared to single suppressor infiltrations. At 9 dpi the level of GFP transcript for single infiltrations with CTV VSRs decreased to low or undetectable levels (Figure 2A). However, for combined CTV co-infiltrations of group 3a, the suppressor activity was still present and GFP mRNA levels were high, with a value 1.6-fold greater compared to the single VSRs (p20 3a and p23 3a).

GFP-specific siRNAs were analysed at 5 dpi by Northern blot using an ambisense GFP-specific probe. Quite abundant accumulation of GFP-specific

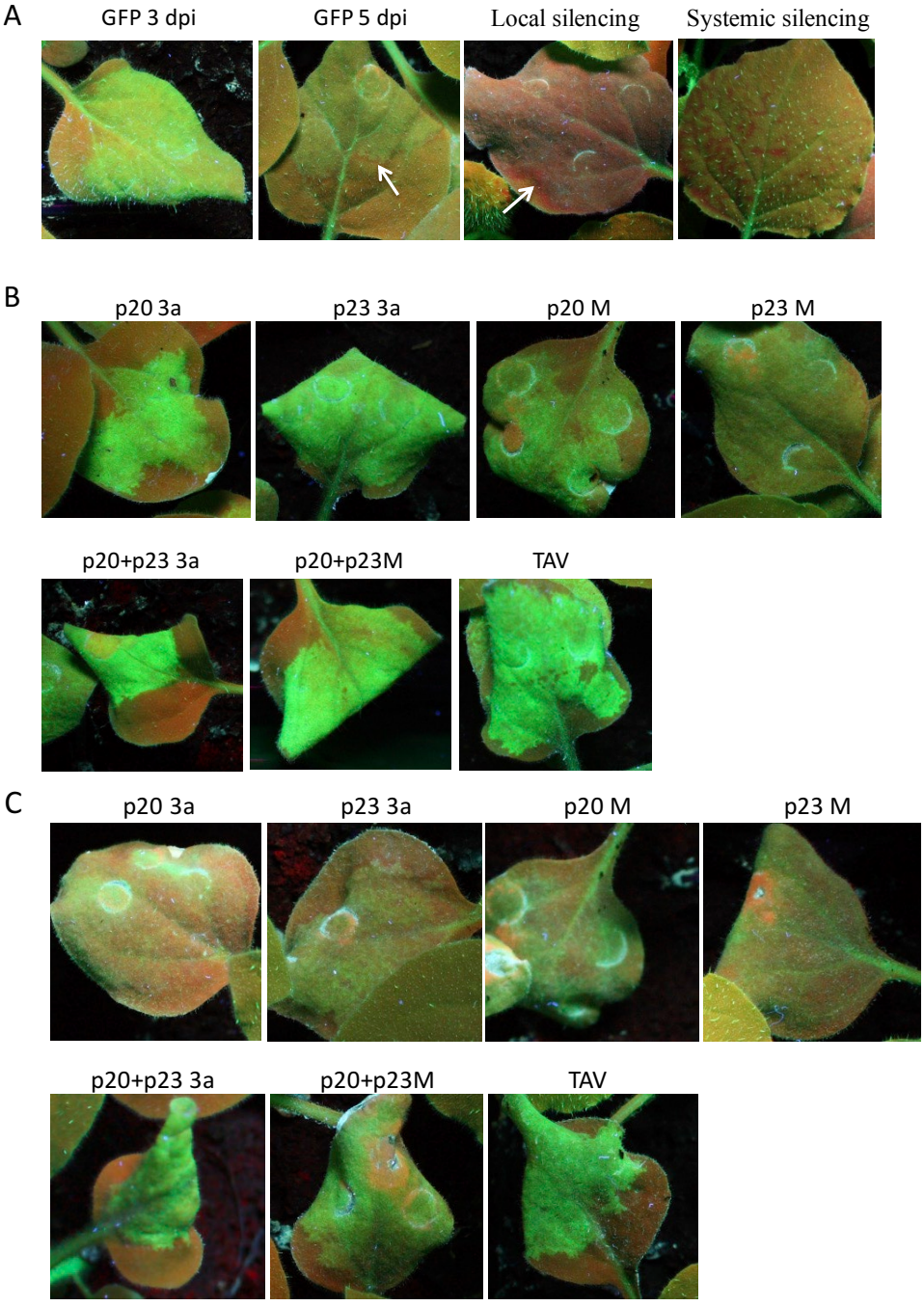

Figure 1. Visual observation of leaves from transgenic *N. benthamiana* 16C plants under UV light at 3, 5 and 9 days post-infiltration (dpi). **A**. Photographs of leaves infiltrated with *Agrobacterium tumefaciens* harbouring pK-GFP alone, showing transient GFP expression at 3 (GFP 3 dpi) and 5 (GFP 5 dpi) dpi, the short-range silencing signal (arrows), local silencing and the systemic silencing. **B**. GFP fluorescence images of leaves after co-infiltration of pK-GFP with TAV, with a single CTV VSR (p20 3a; p23 3a; p20 M; p23 M) and double co-infiltration of each p20 and p23 constructs from group 3a (p20+p23 3a) and group M (p20+p23 M), at 5 dpi. **C**. GFP fluorescence images of leaves after co-infiltration of pK-GFP with TAV, a single CTV VSR (p20 3a; p23 3a; p20 M; p23 M) or double co-infiltration of each p20 and p23 constructs from group 3a (p20+p23 3a) and group M (p20+p23 M), at 9 dpi.

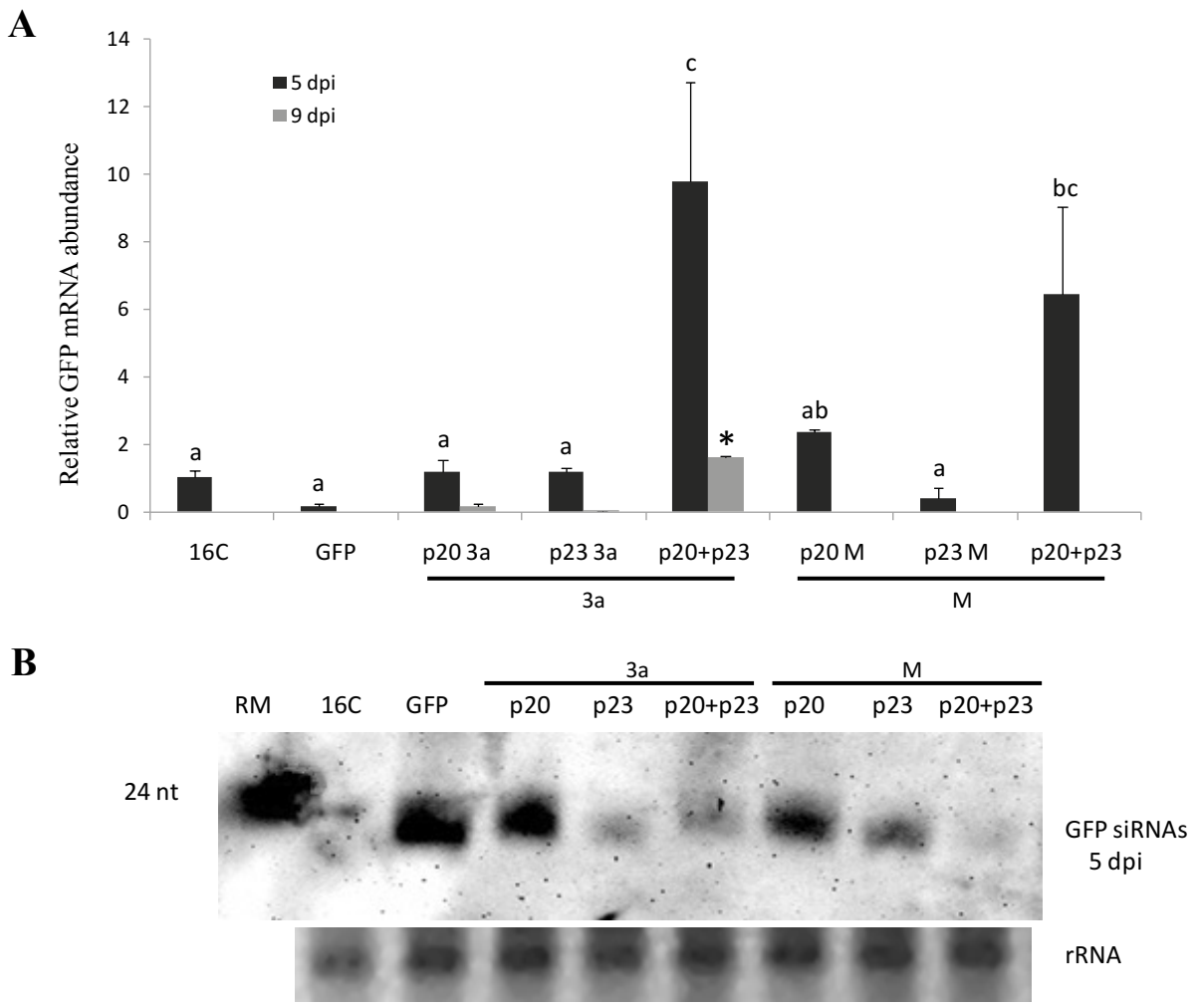

Figure 2. A. Relative levels of GFP mRNA in agro-infiltrated *N. benthamiana* 16C leaves at 5 and 9 dpi, determined by qRT-PCR and normalized against the levels of the *ubiquitin* gene. 16C: 16C non-inoculated plants, used as a reference to assay relative expression. GFP: single infiltration with pK-GFP. p20 3a, p23 3a, p20 M, p23 M: co-infiltration of pK-GFP with the corresponding p20 or p23 construct. p20+p23 3a, p20+p23 M: co-infiltration of pK-GFP with each p20 and p23 constructs of the corresponding viral isolate. Tav-2b: co-infiltration of pK-GFP with the pK-Tav-2b construct. Error bars represent standard deviation (SD) of three independent determinations. Different letters above the bars indicate a statistically significant difference by Tukey´s test at $P<0.05$. Asterisk (*) means a statistically significant difference on the levels of GFP transcripts at 9 dpi, by Tukey´s test at $P<0.05$. **B.** RNA blot analysis of GFP-specific siRNAs extracted from agro-infiltrated *N. benthamiana* 16C leaves at 5 dpi, carrying the correspondent construction(s) indicated above the image. RM: 24-nt synthetic RNA marker. 16C: non-inoculated 16C plants. The bottom panel display the 5S rRNA loading control stained with ethidium bromide.

siRNAs was detected for plants inoculated with pK-GFP, which correlated well with the low levels of GFP mRNA observed. No siRNAs were detected on non-infiltrated 16C plants (Figure 2B). The presence of the CTV suppressors resulted in reduced accumulation of siRNAs and high GFP transcript levels. The low intensity band of siRNAs associated with p23 was not correlated with the expected high levels of GFP mRNA, a discrepancy which cannot be explained (Figure 2B).

Combined action of p20 and p23 results in an enhanced suppressive activity

In order to make clear that the higher suppressive activity found for combined CTV VSRs was not due to an additive effect of the amounts of VSR infiltrated, the co-infiltration of p20 plus p23 was performed with a 0.25 OD_{600}. When both VSRs were co-infiltrated at low OD_{600}, low suppression activity was expected in case there is an additive effect. 16C plants were simultaneously infiltrated with *A. tumefaciens* cultures carrying pK-p20 M, pK-p23 M and pK-GFP at equal OD_{600} of 0.25. The GFP fluorescence of leaves observed at 5 dpi was similar to previous results at 0.5 OD_{600}, both for single or combined VSR constructs (Figure 3A). The combined VSR constructs preserved the greenish patch for more than 9 dpi (data not shown). Rough quantification of the GFP fluorescence intensity in leaves was done for images converted to black and white (Figure 3B). The data showed that local suppression of PTGS was independent of the *A. tumefaciens* culture optical density tested. The double infiltration with constructs pK-p20 plus pK-p23 of Gp M at 0.25 OD_{600} induced GFP brightness comparable to 0.5 OD_{600}. Taken together, these results suggest an enhanced suppressive activity when both proteins p20

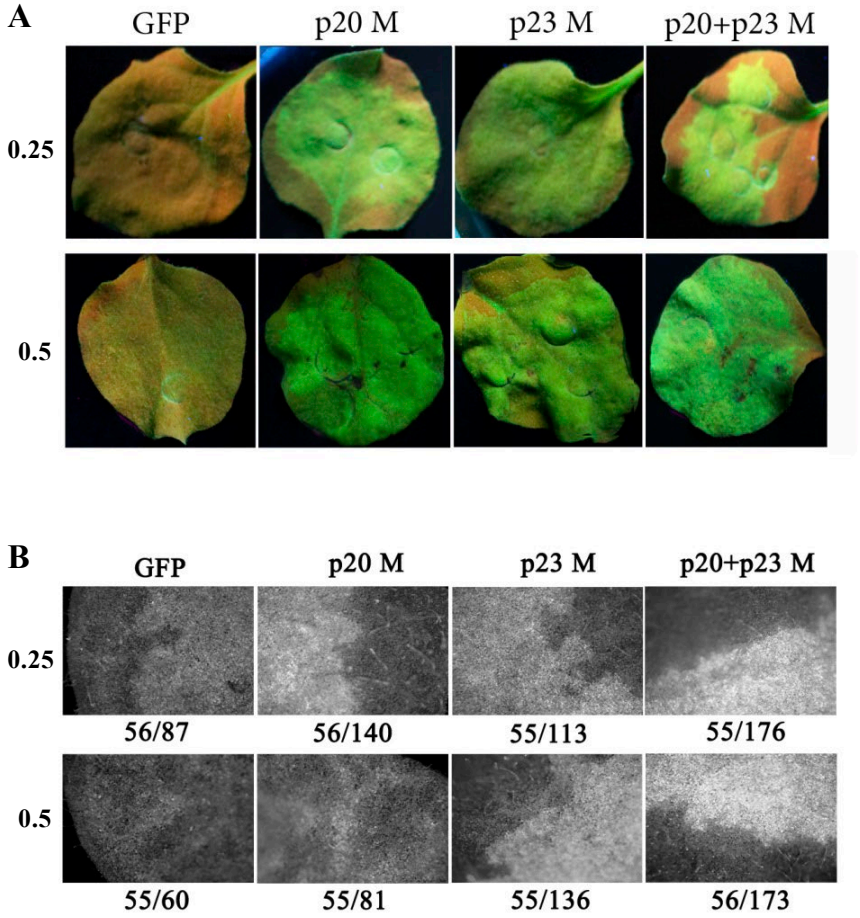

Figure 3. A. The GFP fluorescence images of the infiltrated leaves inoculated with *Agrobacterium* cultures at OD_{600} of 0.25 and 0.5 taken at 5 dpi under UV light. GFP: single infiltration with pK-GFP; p20 M, p23 M: co-infiltration of pK-GFP with the corresponding p20 or p23 constructs; p20+p23 M: co-infiltration of pK-GFP with p20 and p23 constructs of the same CTV isolate. **B.** Graytone images of GFP fluorescence taken under UV light with a stereo microscope from leaves at 5 dpi with the same conditions described at point A. Values below the images correspond to the ratio between red (black areas) and green (bright areas) levels.

and p23 act together, rather than an additive effect of suppressor activity.

Discussion

CTV encodes multiple suppressor proteins that were described to exhibit distinct features in silencing suppression with p20 and p23 proteins targeting the intracellular while CP and p20 target the intercellular silencing mechanism (Lu *et al*., 2004). Since both p20 and p23 target the local RNA silencing mechanism, the present study aimed to compare: a) the activity of these two suppressors, and b) the single activity of each suppressor with the co-expression of both VSRs from the same isolate. P20 and p23 proteins were previously characterized as efficient, but not strong, local silencing suppressors (Marques *et al*., 2012; Costa *et al*., 2014). Assay of p20 suppressors from five isolates belonging to distinct phylogenetic groups showed that they were not able to inhibit short range or systemic spreading of RNA silencing (Marques *et al*., 2012). These studies are not in agreement with the previous report by Lu *et al*. (2004), who, working with a decline isolate (T36) from Florida, found a p20 protein that blocked the intercellular silencing. Moreover, p23 was reported to do not interfere with the production or export of the short-range or the systemic silencing (Lu *et al*., 2004), but p23 expression from a mild stem pitting isolate of Madeira Island (Gp 5) was found to block systemic silencing (Costa *et al*., 2014). Therefore, the suppressor ability of p20 and p23 may vary with the isolate, although our results indicate that this is not related to the symptoms type associated to a particular virus isolate.

In the present study, marked differences for GFP fluorescence were found between leaves infiltrated with p20 or p23 from a mild (Gp M) or a stem pitting isolate (Gp 3a), on local RNA silencing, and both suppressors reduced the amount of GFP siRNAs (Figure 1 and 2B). Also the level of siRNAs in leaves infiltrated with p23 was low compared with p20, along with corresponding low level of GFP transcripts. Expression of p23 from isolate T36 also yielded relatively low levels of siRNAs compared to expression of p20, but in this case deduced by a dissimilar GFP fluorescence (Lu *et al*., 2004). Double suppressor co-infiltrations of CTV VSRs of isolates from Gp 3a and M induced intense GFP fluorescence accompanied by accumulation of GFP mRNA and reduced GFP siRNAs. GFP fluorescence of leaves co-infiltrated with a single suppressor using *A. tumefaciens* cultures at OD_{600} of 0.5 or 0.25 was comparable (Figure 3). The same was observed for double suppressor co-infiltrations at the same OD_{600} values. These findings suggest an enhanced activity when proteins p20 and p23 act together, since the high intensity of GFP fluorescence was independent of the *A. tumefaciens* inoculum, and result from p20 plus p23 co-expression. Synergistic interactions were reported for co-infection of plants by two viruses, associated with the activity of viral suppressors of both viruses on PTGS, which culminate with increased systemic symptoms and high virus titre (Vanitharani *et al*., 2004; Bag *et al*., 2012). The strong antiviral defence system detected in infected Mexican lime and *Citrus sinensis* (L.) Osb. (Ruiz-Ruiz *et al*., 2011; Flores *et al*., 2013) where CTV reaches a high virus titre, is accompanied with a high levels of sRNA (small RNA) production against CTV. This evokes the advantages of CTV carrying two silencing suppressors, not only to enhance viral accumulation in these susceptible hosts, but also to favour cell-to-cell viral movement. Supporting this idea is the observation in the present study that p20 singly or doubly infiltrated with p23 caused a delay in the onset of the short-range signalling. P20 and p23 proteins were already assayed for direct interactions to one another through the two-hybrid system, with no detectable activity (Gowda *et al*., 2000). Nevertheless, these CTV proteins are needed to the development of a systemic infection, which is prevented by deletion of p20 or p23 (Tatineni *et al*., 2008; Dawson *et al*., 2013; Flores *et al*., 2013). This indicates that they have coordinated and complementary activity at diverse levels in a viral infection. P20 and p23 proteins are among the most expressed in infected citrus tissues (Gowda *et al*., 2001). Despite the multiple functions of p23, it is remarkable that the VSR activity is related to most of its nucleotide sequence, which is abolished by several mutations (Ruiz-Ruiz, 2013).

Dissimilar roles were assigned to p20 and p23 not only in viral infection, but also on the RNA silencing mechanism, with molecular targets still unknown. Deep insights into the steps of the antiviral pathway targeted by CTV suppressors is needed to unveil the elaborate strategy of this virus to achieve successful host infection.

Acknowledgements

This study was supported by the grant PTDC/AGR-GPL/99512/2008 from Foundation for Science and Technology, Portugal. Ângela Costa was funded by Foundation for Science and Technology, PhD grant SFRH/BD/62248/2009. The authors thank Florinda Gama for helping with the statistical analyses.

Literature cited

Albiach-Martí M.R., C. Robertson, S. Gowda, S. Tatineni, B. Belliure, S.M. Garnsey, S.Y. Folimonova, P. Moreno and W.O. Dawson, 2010. The pathogenicity determinant of *Citrus tristeza virus* causing the seedling yellows syndrome maps at the 3'-terminal region of the viral genome. *Molecular Plant Pathology* 11, 55–67. (DOI:10.1111/J.1364-3703.2009.00572.X).

Alvarado V. and H.B. Scholthof, 2009. Plant responses against invasive nucleic acids: RNA silencing and its suppression by plant viral pathogens. *Seminars in Cell & Developmental Biology* 20, 1032–1040. (DOI:10.1016/j.semcdb.2009.06.001).

Azevedo J., D. Garcia, D. Pontier, S. Ohnesorge, A. Yu, S. Garcia, L. Braun, M. Bergdoll, M.A. Hakimi, T. Lagrange and O. Voinnet, 2010. Argonaute quenching and global changes in Dicer homeostasis caused by a pathogen-encoded GW repeat protein. *Genes & Development* 24, 904–915. (DOI:10.1101/gad.1908710).

Bag S., N. Mitter, S. Eid and H.R. Pappu, 2012. Complementation between two tospoviruses facilitates the systemic movement of a plant virus silencing suppressor in an otherwise restrictive host. *PLoS ONE* 7, e44803. (DOI:10.1371/journal.pone.0044803).

Baulcombe D., 2004. RNA silencing in plants. *Nature* 431, 356–363. (DOI:10.1038/nature02874).

Brigneti G., O. Voinnet, W.X. Li, L.H. Ji, S.W. Ding and D.C. Baulcombe, 1998. Viral pathogenicity determinants are suppressors of transgene silencing in *Nicotiana benthamiana*. *The Embo Journal* 17, 6739–6746.

Burgyán J., 2008. Role of silencing suppressor proteins. In: *Plant Virology Protocols, from Viral Sequence to Protein Function* (Foster G.D., I.E Johansen., Y. Hong and P.D. Nagy, ed.), Humana Press, Totowa, NJ, USA, 69–79.

Burgyán J. and Z. Havelda., 2011. Viral suppressors of RNA silencing. *Trends in Plant Science*. 16, 265–272. (DOI:10.1016/j.tplants.2011.02.010).

Canizares M.C., J. Navas-Castillo and E. Moriones, 2008. Multiple suppressors of RNA silencing encoded by both genomic RNAs of the crinivirus, *Tomato chlorosis virus*. *Virology* 379, 168–174. (DOI:10.1016/j.virol.2008.06.020).

Chun-zhen C., Jia-wei, Y., Hu-bin, Y., Xue-jun, B, Yong-yan, Z., Zhi-ming, L. and Z. Guang-yan, 2015. Expressing p20 hairpin RNA of *Citrus tristeza virus* confers *Citrus aurantium* with tolerance/resistance against stem pitting and seedling yellow CTV strains. *Journal of Integrative Agriculture* 14(9), 1767–1777. (DOI: 10.1016/S2095-3119(14)60937-0).

Costa Â., N. Marques and G. Nolasco, 2014. *Citrus tristeza virus* p23 may suppress systemic silencing but is not related to the kind of viral syndrome. *Physiological and Molecular Plant Pathology* 87, 69–75.

Dawson W.O., S.M. Garnsey, S. Tatineni, S.Y. Folimonova, S.J. Harper and S. Gowda, 2013. *Citrus tristeza virus*-host interactions. *Frontiers in Microbiology* 4, 88. (DOI:10.3389/fmicb.2013.00088).

Diaz-Pendon J.A. and S.W. Ding, 2008. Direct and indirect roles of viral suppressors of RNA silencing in pathogenesis. *Annual Review of Phytopathology* 46, 303–326. (DOI:10.1146/annurev.phyto.46.081407.104746).

Ding S.W., 2010. RNA-based antiviral immunity. *Nature Reviews Immunology* 10, 632–644. (DOI:10.1038/nri2824).

Dolja V.V., J.F. Kreuze and J.P. Valkonen, 2006. Comparative and functional genomics of closteroviruses. *Virus Research* 117, 38–51. (DOI:10.1016/j.virusres.2006.02.002).

Fagoaga C., C. López, P. Moreno, L. Navarro, R. Flores and L. Peña, 2005. Viral-like symptoms induced by the ectopic expression of the p23 gene of *Citrus tristeza virus* are citrus specific and do not correlate with the pathogenicity of the virus strain. *Molecular Plant-Microbe Interactions Journal* 18(5), 435–445. (DOI: 10.1094/MPMI -18-0435).

Fagoaga C., G. Pensabene-Bellavia, P. Moreno, L. Navarro, R. Flores and L. Peña, 2011. Ectopic expression of the p23 silencing suppressor of *Citrus tristeza virus* differentially modifies viral accumulation and tropism in two transgenic woody hosts. *Molecular Plant Pathology* 12, 898–910.

Flores R., S. Ruiz-Ruiz, N. Soler, J. Sanchez-Navarro, C. Fagoaga, C. Lopez, L. Navarro, P. Moreno and L. Peña, 2013. *Citrus tristeza virus* p23: a unique protein mediating key virus-host interactions. *Frontiers in Microbiology* 4, 1–9. (DOI:10.3389/fmicb.2013.00098).

Ghorbel R., C. López, C. Fagoaga, P. Moreno, L. Navarro, R. Flores and L. Peña, 2001. Transgenic citrus plants expressing the *Citrus tristeza virus* p23 protein exhibit viral-like symptoms. *Molecular Plant Pathology* 2, 27–36.

Giner A., L. Lakatos, M. Garcia-Chapa, J.J. Lopez-Moya and J. Burgyan, 2010. Viral protein inhibits RISC activity by argonaute binding through conserved WG/GW motifs. *PLoS Pathogens* 6, e1000996. (DOI:10.1371/journal.ppat.1000996).

Glick E., A. Zrachya, Y. Levy, A. Mett, D. Gidoni, E. Belausov, V. Citovsky and Y. Gafni, 2008. Interaction with host SGS3 is required for suppression of RNA silencing by *Tomato yellow leaf curl virus* V2 protein. *Proceedings of the National Academy of Sciences of the USA* 105, 157–161. (DOI:10.1073_pnas.0709036105).

Gowda S., T. Satyanarayana, C.L. Davis, J. Navas-Castillo, M.R. Albiach-Martí, M. Mawassi, N. Valkov, M. Bar-Joseph, P. Moreno and W.O. Dawson, 2000. The p20 gene product of *Citrus tristeza virus* accumulates in the amorphous inclusion bodies. *Virology* 274, 246–254. (DOI:10.1016/j.pmpp.2014.07.002).

Gowda S., T. Satyanarayana, M.A. Ayllón, M.R. Albiach-Martí, M. Mawassi, S. Rabindran, S.M. Garnsey and W. Dawson, 2001. Characterization of the cis-acting elements controlling subgenomic mRNAs of *Citrus tristeza virus*:

production of positive- and negative-stranded 3′-terminal and positive-stranded 5′-terminal RNAs. *Virology* 286, 134–151. (DOI:10.1006/viro.2001.0987).

Haseloff J., K.R. Siemering, D.C. Prasher and S. Hodge, 1997. Removal of a cryptic intron and subcellular localization of green fluorescent protein are required to mark transgenic *Arabidopsis* plants brightly. *Proceedings of the National Academy of Sciences of the USA* 94, 2122-2127.

Herr A.J. and D.C. Baulcombe, 2004. RNA silencing pathways in plants. *Cold Spring Harbor Symposia on Quantitative Biology* 69, 363–370.

Himber C., P. Dunoyer, P. Moissiard, C. Ritzenthaler and O. Voinnet, 2003. Transitivity-dependent and -independent cell-to-cell movement of RNA silencing. *The Embo Journal* 22, 4523–4533.

Karasev A.V., V.P. Boyko, S. Gowda, O.V. Nikolaeva, M.E. Hilf, E.V. Koonin, C.L. Niblett, K. Cline, D.J. Gumpf, R.F. Lee, S.M. Garnsey, D.J. Lewandowski and W.O. Dawson, 1995. Complete sequence of the *Citrus tristeza virus* RNA genome. *Virology* 208, 511–520.

Karimi M., D. Inze and A. Depicker, 2002. Gateway vectors for *Agrobacterium*-mediated plant transformation. *Trends in Plant Science* 7, 193–195.

Kasschau K.D., Z. Xie, E. Allen, C. Llave, E.J. Chapman, K.A. Krizan, J.C. Carrington, 2003. P1/HC-Pro, a viral suppressor of RNA silencing, interferes with *Arabidopsis* development and miRNA function. *Developmental Cell* 4, 205–217.

Lopez C., J. Navas-Castillo, S. Gowda, P. Moreno and R. Flores, 2000. The 23-kDa protein coded by the 3′-terminal gene of *Citrus tristeza virus* is an RNA-binding protein. *Virology* 269, 462–470. (DOI:10.1006/viro.2000.0235).

Lu R., A. Folimonov, M. Shintaku, W-X. Li, B.W. Falk, W.O. Dawson and S-W. Ding, 2004. Three distinct suppressors of RNA silencing encoded by a 20-kb viral RNA genome. *Proceedings of the National Academy of Sciences of the USA* 101, 15742–15747. (DOI:10.1073_pnas.0404940101).

MacDiarmid R., 2005. RNA silencing in productive virus infections. *Annual Review of Phytopathology* 43, 523–544. (DOI:10.1146/annurev.phyto.43.040204.140204).

Maghuly F., R.C. Ramkat and M. Laimer, 2014. Virus versus host plant microRNAs: who determines the outcome of the interaction? *PLoS ONE* 9, e98263. (DOI:10.1371/journal.pone.0098263).

Marques N.T., A.A. Costa, D. Lopes, G. Silva and G. Nolasco, 2012. Comparing p20's RNA silencing suppressing activity among five phylogenetic groups of *Citrus tristeza virus*. *European Journal of Plant Pathology* 133, 229–235. (DOI:10.1007/s10658-011-9877-0).

Merai Z., Z. Kerenyi, S. Kertesz, M. Magna, L. Lakatos and D. Silhavy, 2006. Double-stranded RNA binding may be a general plant RNA viral strategy to suppress RNA silencing. *Journal of Virology* 80, 5747–5756. (DOI:10.1128/JVI.01963-05).

Moreno P., S. Ambros, M.R. Albiach-Martí, J. Guerri and L. Peña, 2008. *Citrus tristeza virus*: a pathogen that changed the course of the citrus industry. *Molecular Plant Pathology* 9, 251–268. (DOI: 10.1111/J.1364-3703.2007.00455.X).

Navas-Castillo J., M. R. Albiach-Martí, S. Gowda, M.E. Hilf, S.M. Garnsey and W.O. Dawson, 1997. Kinetics of accumulation of *Citrus tristeza virus* RNAs. *Virology* 228, 92–97.

Nolasco G., C. Santos, G. Silva and F. Fonseca, 2009. Development of an asymmetric PCR-ELISA typing method for *Citrus tristeza virus* based on the coat protein gene. *Journal of Virological Methods* 155, 97–108. (DOI:10.1016/j.jviromet.2008.09.030).

Pall G.S., C. Codony-Servat, J. Byrne, L. Ritchie and A. Hamilton, 2007. Carbodiimide-mediated crosslinking of RNA to nylon membranes improves the detection of siRNA, miRNA and piRNA by Northern blot. *Nucleic Acids Research* 35, e60. (DOI:10.1093/nar/gkm112).

Pallas V. and J.A. García, 2011. How do plant viruses induce disease? Interactions and interference with host components. *Journal of General Virology* 92, 2691–2705. (DOI:10.1099/vir.0.034603-0).

Pfaffl M.W., 2001. A new mathematical model for relative quantification in real-time RT-PCR. *Nucleic Acids Research* 29(9), e45.

Rawlings R.A., V. Krishnan and N.G. Walter, 2011. Viral RNAi suppressor reversibly binds siRNA to outcompete Dicer and RISC via multiple turnover. *Journal of Molecular Biology* 408, 262–276. (DOI:10.1016/j.jmb.2011.02.038).

Rotenberg D., T.S. Thompson, T.L. German and D.K. Willis, 2006. Methods for effective real-time RT-PCR analysis of virus-induced gene silencing. *Journal of Virological Methods* 138, 49–59. (DOI:10.1016/j.jviromet.2006.07.017).

Ruiz-Ruiz S., B. Navarro, A. Gisel, L. Penã, L. Navarro, P. Moreno, F. Di Serio and R. Flores, 2011. *Citrus tristeza virus* infection induces the accumulation of viral small RNAs (21–24-nt) mapping preferentially at the 30-terminal region of the genomic RNA and affects the host small RNA profile. *Plant Molecular Biology* 75, 607–619. (DOI:10.1007/s11103-011-9754-4).

Ruiz-Ruiz S., N. Soler, J. Sanchez-Navarro, C. Fagoaga, C. López, L. Navarro, P. Moreno, L. Peña and R. Flores, 2013. *Citrus tristeza virus* p23: determinants for nucleolar localization and their influence on suppression of RNA silencing and pathogenesis. *Molecular Plant-Microbe Interactions* 26, 306–318. (DOI:10.1094/MPMI-08-12-0201-R).

Satyanarayana T., S. Gowda, M.A. Ayllón, M.R. Albiach-Martí, S. Rabindran and W.O. Dawson, 2002. The p23 protein of *Citrus tristeza virus* controls asymmetrical RNA accumulation. *Journal of Virology* 76, 473–483. (DOI:10.1128/JVI.76.2.473–483.2002).

Satyanarayana T., S. Gowda, M. Mawassi, M.R. Albiach-Martí, M.A. Ayllón, C. Robertson, S.M. Garnsey and W.O. Dawson, 2000. Closterovirus encoded HSP70 homolog and p61 in addition to both coat proteins function in efficient virion assembly. *Virology* 278, 253–265. (DOI:10.1006/viro.2000.0638).

Schott G., A. Mari-Ordonez, C. Himber, A. Alioua, O. Voinnet and P. Dunoyer, 2012. Differential effects of viral silencing suppressors on siRNA and miRNA loading support the existence of two distinct cellular pools of ARGONAUTE1. *The Embo Journal* 31, 2553–2565. (DOI:10.1038/emboj.2012.92).

Senshu H., Y. Yamaji, N. Minato, T. Shiraishi, K. Maejima, M. Hashimoto, C. Miura, Y. Neriya and S. Namba, 2011. A dual strategy for the suppression of host antiviral silenc-

ing: two distinct suppressors for viral replication and viral movement encoded by *Potato virus M*. *Journal of Virology* 85, 10269–10278. (DOI:10.1128/JVI.05273-11).

Silhavy D., A. Molnár, A. Lucioli , G. Szittya, C. Hornyik, M. Tavazza and J. Burgyán, 2002. A viral protein suppresses RNA silencing and binds silencing-generated, 21- to 25-nucleotide double-stranded RNAs. *The Embo Journal* 21, 3070–3080.

Silva G., 2011. Phylodynamics of *Citrus tristeza virus*: molecular epidemiology and biological evolution (written in portuguese). PhD Thesis, Faculdade de Ciências e Tecnologia, Universidade do Algarve, Faro, Portugal, 142 pp.

Soler N., C. Fagoaga, C. López, P. Moreno, L. Navarro, R. Flores and L. Peña, 2015. Symptoms induced by transgenic expression of p23 from *Citrus tristeza virus* in phloem-associated cells of Mexican lime mimic virus infection without the aberrations accompanying constitutive expression. *Molecular and Plant Pathology* 16(4), 388–399. (DOI: 10.1111/mpp.12188).

Szittya G., T. Dalmay and J. Burgyán, 2008. Plant Antiviral Defense: Gene Silencing Pathway. In: *Desk Encyclopedia of Plant and Fungal Virology* (Mahy B.W.J. and M.H.V. Regenmortel, ed.). 1st ed. Academic Press, Oxford, UK, 30–38. (DOI:10.1371/journal.ppat.1000838).

Tatineni S., C.J. Robertson, S.M. Garnsey, M. Bar-Joseph, S. Gowda and W.O. Dawson, 2008. Three genes of *Citrus tristeza virus* are dispensable for infection and movement throughout some varieties of citrus trees. *Virology* 376, 297–307. (DOI:10.1016/j.virol.2007.12.038).

Valli A., J.C. Oliveros, A. Molnar, D. Baulcombe and J.A. Garcia, 2011. The specific binding to 21-nt double-stranded RNAs is crucial for the anti-silencing activity of *Cucumber vein yellowing virus* P1b and perturbs endogenous small RNA populations. *RNA* 17, 1148–1158. (DOI:10.1261/rna.2510611).

Vanitharani R., P. Chellappan, J.S. Pita and C.M. Fauquet, 2004. Differential roles of AC2 and AC4 of cassava geminiviruses in mediating synergism and suppression of posttranscriptional gene silencing. *Journal of Virology* 78, 9487–9498. (DOI: 10.1128/JVI.78.17.9487–9498.2004).

Voinnet O., 2001. RNA silencing as a plant immune system against viruses. *Trends in Genetics* 17, 449–459.

Yaegashi H., T. Takahashi, M. Isogai, T. Kobori, S. Ohki and N. Yoshikawa, 2007. *Apple chlorotic leaf spot virus* 50 kDa movement protein acts as a suppressor of systemic silencing without interfering with local silencing in *Nicotiana benthamiana*. *Journal of General Virology* 88, 316–324. (DOI:10.1099/vir.0.82377-0).

Yoon J.Y., K.S. Han, H.Y. Park and S.K. Choi, 2012. Comparative analysis of RNA silencing suppression activities between viral suppressors and an endogenous plant RNA-dependent RNA polymerase. *Virus Genes* 44, 495–504. (DOI:10.1007/s11262-012-0725-x).

Accepted for publication: February 14, 2016
Published online: July 29, 2016